Pergamon

Progress in Surface Science, Vol. 59, No. 1–4, pp. 135–147, 1998

Printed in Great Britain
0079-6816/98 $19.00

PII: S0079-6816(98)00041-0

DENSITY-FUNCTIONAL THEORY STUDIES ON MICROSCOPIC PROCESSES OF GaAs GROWTH

PETER KRATZER, CAROLINE G. MORGAN[1] and MATTHIAS SCHEFFLER

Fritz-Haber-Institut der Max-Planck-Gesellschaft, 14195 Berlin, Germany

Abstract

Results for the elementary processes of MBE growth of GaAs on the frequently used GaAs(001) substrate are reviewed. We propose a bottom-up approach, where a growth model is constructed from the results of density functional theory (DFT) calculations. The implications of such a model can be tested against the information from STM images. First, the stable surface reconstructions are reviewed. Under the most commonly used conditions for MBE growth, the arsenic-rich $\beta 2$ (2×4) reconstruction, which contains As dimers as basic building blocks, is the most stable. Next, the adsorption and diffusion of Ga atoms and As molecules on this surface is described. The DFT calculations support the picture that adsorbed Ga atoms are quite stable against re-evaporation. Thus, their mobility determines the homogeneity of the growing layer. Incorporation of Ga atoms proceeds by splitting the As dimers. We propose a model where growth proceeds in two stages: filling of trenches in the $\beta 2$ (2×4) reconstruction, followed by nucleation of islands on the surface regions where the trenches are filled. We demonstrate how clusters of incorporated Ga atoms act as nuclei for the process of trench filling. Concerning island formation, the role of step formation energies and attachment probabilities of mobile adatoms at steps is discussed. Knowledge of these is crucial for an understanding of island shapes. Ongoing research is aiming at understanding of the microscopic mechanisms giving rise to the transition between the step-flow mode and the island-nucleation mode of growth.

1. Introduction

In recent years, there has been considerable interest in semiconductor devices built from structures which have lateral dimensions of about ten to twenty nanometers. Such structures allow the electric carriers to be confined, so that they can only move in one dimension (quantum

[1]Permanent address: Wayne State University, Detroit, MI, USA

wires) or zero dimensions (quantum dots). To fabricate these structures in larger numbers, it is highly desirable to exploit the natural properties of the growth process, which—under appropriate conditions—can lead to self-organization and spontaneous formation of nanostructures. For instance, Kapon and co-workers [1] managed to create quantum wires on a substrate with mesoscopic grooves by exploiting the different growth properties of GaAs and AlGaAs at the bottom of these grooves. Another example is the appearance of quantum dots in heteroepitaxial growth of materials with a lattice mismatch. The formation of lattice-matched and defect-free islands, the so-called coherent islands, is believed to be largely determined by growth kinetics [2,3]. For a better understanding of these phenomena, we need to obtain insight into the processes of growth on a microscopic scale.

In the past, growth simulations for the III-V compounds have mainly been based on semiempirical models. These are mostly variants of the so-called solid-on-solid (SOS) model with a bond-strength bond-order description of the covalent bonds between atoms. In the simplest case, only one component (Ga) is treated, and diffusion is modeled on a simple cubic lattice [4,5]. In recent years, the model has been extended to include the physical cation (fcc) lattice [6], some kinetic aspects of arsenic adsorption [7], or a Schwoebel-Ehrlich barrier [8]. Generally, the parameters of these models (e.g., bond strengths) are "tuned" to reproduce experimental results, like the oscillations observed in RHEED. Only very recently, more sophisticated growth models have been developed using the information of STM pictures as additional input [9]. However, with the more refined models, the need arises to fix the growing number of parameters from additional sources of information. Still, several microscopic processes, e.g., adatom hopping, are lumped together into effective parameters, like an effective barrier for diffusion. Here, we face the difficulty in assigning the effective parameters of these models to specific microscopic processes.

In the present article, we pursue a complementary approach, starting from the microscopic processes: density functional theory (DFT) is used to determine the geometry and total energy of numerous microscopic configurations with the help of large-scale electronic structure calculations. In this way, the relevant processes and parameters of a growth model can be determined from first principles. The results of the calculations can be checked against the information extracted from STM images of growing surfaces. We also compare results obtained within the local-density approximation (LDA) for the exchange-correlation functional [10] with those obtained within the generalized-gradient approximation (GGA) in its latest version [11]. While the first functional has been a standard in DFT calculations for many years, the latter gives an improved description of the adsorption of atoms and small molecules. For further technical aspects of these calculations,

which have become a very powerful and versatile research tool during the last decade, we refer to the literature [12,13].

In this article, we will limit ourselves to the MBE growth of GaAs from the elements. The process of MOCVD growth is clearly more complicated. Thus, a first-principles theoretical modeling has not been attempted yet. The following sections will review the experimental and theoretical information available for the elementary steps of MBE growth, such as deposition, diffusion, island nucleation, and growth in the step-flow mode. Moreover, some new results from DFT calculations will be presented.

2. GaAs(001) Surface

A substrate particularly well suited for the growth of GaAs is the (001) surface. Since diffusion barriers are quite high on GaAs surfaces (see below), temperatures up to 850 K are used for growing relatively smooth layers. On the (001) surface, the sticking coefficient for Ga atoms and As molecules is between 0.1 and 1 even in this temperature range [14,15]. The growing surface displays a large variety of reconstructions, depending on growth temperature and the ratio of Ga and As fluxes [16]. By means of electron diffraction under grazing incidence (RHEED), the symmetry properties of the surface can be studied *in situ* during growth. For more information on the atomic configurations, STM studies can be very helpful [17]. However, this technique requires quenching of the growing substrate. Additional information to decide between competing structure models is provided by DFT calculations.

To determine which surface structures are the most stable ones after growth of a new layer, we take the point of view of equilibrium thermodynamics. The most stable reconstruction is identified by the minimum of the surface free enthalpy at a given temperature and pressure. Although the structures observed during growth are, in general, non-equilibrium structures, knowledge of the equilibrium structures is a necessary starting point for any further considerations. Moreover, it is often possible to prepare the equilibrium structures by careful annealing of the samples. The thermodynamic phase rules for a two-component system like GaAs require the existence of an additional thermodynamic variable, which governs the chemical composition of the surface. We can choose this variable to be the chemical potential of one of the elements, for instance of arsenic. The chemical potential of As can be changed experimentally by changing the As_2 partial pressure in the growth chamber.

For zero temperature, surface energies of various reconstructions have been calculated [18,19]. Those with the lowest surface energy (depending on As pressure), the $\beta 2$ (2×4) reconstruction and the c(4×4) reconstruction, both contain arsenic surface dimers as the basic structural unit. While the c(4×4) reconstruction is most relevant for the As-rich conditions in MOCVD growth, we will concentrate here on the $\beta 2$ (2×4) reconstruction, which prevails under the temperature and pressure conditions of high-temperature MBE processes. The latter reconstruction is characterized by a missing row of Ga atoms in the last Ga layer, which leads to "trenches" on the surface, running in the $[\bar{1}10]$ direction. Arsenic atoms in the trenches form dimers. Two parallel As dimers in the topmost layer separate the trenches (see Fig. 1a).

There are other (2×4) reconstructions which are only slightly higher in surface energy, and are expected to play a role as intermediate stages during growth. By adding two Ga atoms per unit cell in the trench, the α reconstruction (Fig. 1b) is obtained. Further addition of two As atoms eventually leads to the β structure (Fig. 1c).

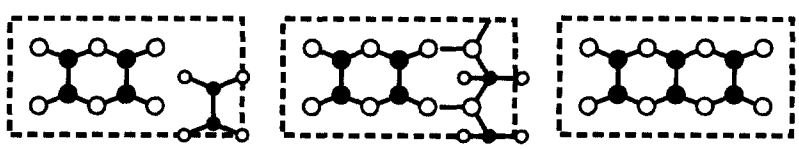

Fig. 1. Sketches of the atomic geometries (top view) for the $\beta 2$, α, and β (2×4) reconstructions of the GaAs(001) surface (from left to right), forming a possible growth sequence. As atoms are black, Ga atoms are white. Decreasing size of the symbols indicates atoms in deeper layers.

3. Deposition and Desorption

Adsorption of gallium atoms and arsenic molecules at the surface is the first step in MBE growth. By means of DFT calculations, the most stable adsorption site and the binding energy can be determined. On the $\beta 2$ reconstructed surface, Ga atoms most favorably adsorb in the trenches. Kley, Ruggerone and Scheffler [20] have determined adsorption sites using the GGA functional. The substrate atoms were allowed to relax after deposition of a Ga adatom. For an unchanged bonding topology of the substrate atoms, they found a stable adsorption site between two adjacent As trench dimers (see Fig. 2 for illustration). We refer to these adatoms as the mobile Ga species, with adsorption energy E_{mobile} (see Table 1). Alternatively, the Ga atom may

split an As dimer in the trench or in the top layer and adsorb in a two-fold coordinated site with adsorption energy E^{II}_{trench} or E^{II}_{top}, respectively. These sites are much more strongly bound and already constitute the first step to incorporation of the Ga atom. Additionally, we consider here splitting of an As trench dimer with subsequent bond formation to one side wall of the trench, which brings the Ga atom into a three-fold coordinated site with adsorption energy E^{III}_{trench}.

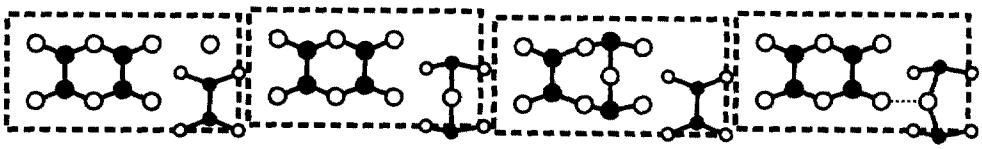

Fig. 2. Schematics for the adsorption sites of Ga on the GaAs(001) $\beta 2$ surface (from left to right): mobile Ga adatom between As dimers in the trench, two-fold coordinated Ga adatom splitting an As trench dimer, two-fold coordinated Ga adatom splitting an As dimer in the top layer, and three-fold coordinated Ga adatom in the trench with additional bond to one side wall.

Adsorption energies calculated with different density functionals for these sites are summarized in Table 1. All calculations were done with a slab consisting of seven atomic layers and a 4×4 lateral unit cell. The bottom layer was passivated with pseudo-hydrogen atoms, and the top six layers and the adatom were allowed to relax. The adsorption energies obtained in LDA are 0.5 eV to 0.9 eV larger than those obtained with the gradient-corrected functional. Moreover, the preference for three-fold or two-fold coordination depends, to some extent, on the functional used. It is well known that the LDA functional favours higher coordination and overestimates

TABLE 1. Adsorption energies of Ga atoms as mobile surface species and incorporated at various sites (in eV, relative to a spin-polarized gas-phase Ga atom). Roman superscripts indicate the local coordination.

	E_{mobile}	E^{II}_{trench}	E^{III}_{trench}	E^{II}_{top}
GGA	−1.5	−2.1	−1.9	−1.9
LDA	−2.2	−2.6	−2.8	−2.5

adsorption energies, while the gradient-corrected results are in better agreement with experimental data. Hence, we believe that the results obtained with the gradient-corrected functional are more reliable, and these numbers will be used in the further discussion.

For the β reconstruction of GaAs(001), the adsorption of Ga atoms has been investigated by Shiraishi [21]. His calculations show that the preferred adsorption site is between two As dimers, similar to the results found for the $\beta 2$ reconstruction. The possibility of splitting of As dimer bonds was not considered in his calculations.

As sources of arsenic in MBE growth, both As_2 and As_4 molecular beams are in use. Since the most important surface reconstructions are built up from As dimers, it is plausible that As_2 adsorbs undissociated. Only in later stages of growth, when a new layer is formed on top of these As dimers, will they break up, due to a reaction with Ga adatoms. For As_4, the reactive sticking coefficient never exceeds 1/2 [22], suggesting that the adsorption reaction is associated with the break-up of the molecule, most likely into two As_2 fragments, only one of which gets adsorbed. This picture is corroborated by the observation that desorption of As_4 is second order with respect to the incident arsenic dose at low fluxes and temperatures in the range of 450–600 K [22], which can be rationalized as the recombinative desorption of two As_2-units at the surface. At present, *ab initio* information on arsenic adsorption is available only for the simpler case of As_2 [23,24]. The binding energy of chemisorbed As_2 depends very much on the local environment. On an ideal $\beta 2$-reconstructed surface, an arsenic dimer is bound by 1.65 eV [23]. However, if two Ga adatoms per (2×4) unit cell have been pre-adsorbed, the binding energy increases to 2.5 eV [23]. A similar increase of the binding energy of As_2 molecules with Ga coverage was also found in the calculations for the β-reconstructed surface [24].

We can estimate desorption rates from the calculated binding energies by assuming a prefactor of $\sim 10^{13}$ s^{-1} in the rate law. The following picture evolves from such an estimate: Ga atoms in two-fold or three-fold coordinated sites are adsorbed sufficiently strongly, so that the rate of desorption is smaller than the incident flux of Ga atoms under typical conditions, and desorption of Ga can be neglected at all but the highest temperatures, up to 900 K. For arsenic, on the other hand, the loss by desorption from the surface can be substantial. At temperatures above 800 K, the adsorption sites will only be replenished from the molecular beam if they form a complex with two extra Ga adatoms. This is consistent with the experimental observation that arsenic incorporation at these temperatures only proceeds when the surface is simultaneously exposed to a Ga beam providing excess Ga adatoms on the surface [14].

4. Diffusion

Since adsorbed Ga atoms are likely to stay on the surface, Ga surface diffusion is crucial for the smoothing out of inhomogeneities introduced by the deposition process, and the growth of high-quality, smooth layers. However, experimental information on the diffusion process is scarce. The experimental derivation of diffusion constants is usually quite indirect and requires interpretation of the data on the basis of some growth model. Here, DFT calculations allow us to identify individual hopping processes and to calculate the diffusivity from them.

When the Brownian motion of a diffusing adatom is slow on the time scale of the substrate phonons, all the information required to determine the diffusion tensor is contained in the potential energy surface (PES) of the moving adatom. The diffusion rates are related to the lowest diffusion barriers, which are found after relaxing the substrate for each lateral position of the adatom. For Ga diffusion on the $\beta 2$ reconstruction of GaAs(001), the PES has been calculated by Kley, Ruggerone and Scheffler [20]. They find that the diffusion is anisotropic, with lower diffusion barriers for the adatom motion along the trenches than for diffusion between trenches. In a similar way, the PES for diffusion on the β reconstruction has been calculated by Shiraishi [21].

The diffusion tensor can be derived by mapping the PES with its binding sites and saddle points onto a discrete network. The links in this network are identified with individual hopping rates, which can be determined from first principles. Under generally applicable assumptions (diffusion barrier $\gg k_B T$, neglect of recrossing trajectories), the rates are described by transition state theory. If a single microscopic process dominates the rate over a range of temperatures, diffusion follows Arrhenius' law in this temperature interval. To calculate the activation energy and the prefactor for an individual process from first principles, one needs to know the relative energies on the PES and the normal mode frequencies at the binding site and at the saddle point site. For a correct determination of the diffusion tensor, the incorporation of Ga atoms into the As dimers must be taken into account. An exact analysis on the basis of the network description gives the following results for diffusion along the [110] direction (perpendicular to the trenches) and along the $[\bar{1}10]$ direction (along the trenches):

$$
\begin{aligned}
D_{[110]} &= 0.1\,\mathrm{cm}^2/\mathrm{s}\ \exp[-1.5\,\mathrm{eV}/k_B T]\,, \\
D_{[\bar{1}10]} &= 0.07\,\mathrm{cm}^2/\mathrm{s}\ \exp[-1.2\,\mathrm{eV}/k_B T]\,.
\end{aligned}
$$

At present, little is known about the diffusion of As species on the surface. STM images of samples annealed at different temperatures show different densities of structural defects, mainly kinks in the As dimer rows [25]. At higher temperatures, the samples become nearly free of such kinks, and the reconstruction is surprisingly well reproduced in the newly grown layer. From this observation, it appears that As dimers could have at least some short range mobility on the surface, e.g., hopping between adjacent binding sites should be possible, which helps to heal some of the defects introduced during growth. However, since arsenic is more weakly bound than Ga, we expect that a substantial contribution to material transport is due to desorption of As_2 (possibly into some mobile precursor state), and re-adsorption at some other, more favourable sites at the surface.

5. Nucleation and Island Growth

From the atomistic point of view, it is exciting to see how the Ga and As atoms of a newly grown layer manage to arrange themselves in order to recover the $\beta 2$ reconstruction. It was already understood in early growth models [26] that different reconstructions may appear locally on the growing surface, acting as metastable intermediates before a newly grown layer is completed. Only with the help of very detailed STM studies [27] it has become possible to refine our understanding of the elementary steps of growth [9]. From the STM pictures, we can conclude that growth on the $\beta 2$-reconstructed surface proceeds in two major steps: filling of the trenches and formation of small islands, which become part of the top-layer As dimers in the new layer. We have studied the trench filling process in great detail by means of *ab initio* calculations [28]. The (4×4) unit cell used in the calculations offers four binding sites for Ga atoms in the trenches. The adsorption energy at low Ga coverages is determined by placing a single Ga adatom in the most stable adsorption site (see Table 1). This corresponds to Ga atoms separated by three empty sites (Ga*** in the notation used in Table 2, with the stars denoting empty sites). We can study the interaction of Ga adatoms by increasing the coverage. Eventually, Ga adatoms will cluster, forming Ga–As–Ga... chains in $[\bar{1}10]$ direction from the As dimers in the trenches (see Fig. 3). Similarly, such chains can be formed from the As dimers of the top layer. The binding energies of these clusters (with respect to a single adatom per unit cell) is shown in Table 2. Although the Ga atoms do not form bonds with each other, the interaction energy can be sizeable, because the Ga adatoms will split one or two As dimers at the bottom of the trenches, depending on their distance (see Fig. 3). For this reason, a pair of Ga atoms, which

induces a local α reconstruction, is already quite stable. By adsorption of arsenic, this structure will be transformed to the even more stable β reconstruction. Ga adsorption in the top-layer As dimers is energetically less favourable (see Table 1), and clustering of Ga in the top layer is distinctly favoured over individual adatoms only for cluster sizes of at least three atoms (see the right column in Table 2). Hence, nucleation of the next layer will start only after the adsorption sites in the trenches are locally occupied. This is consistent with the experimental observation [27].

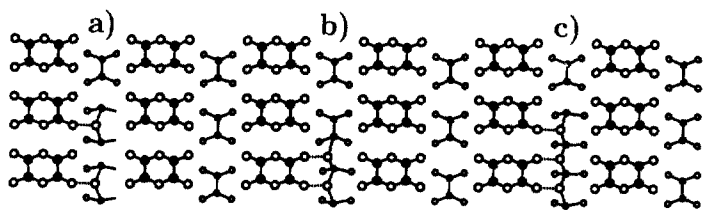

Fig. 3. "Trench" adsorption geometries (cf. respective column in Table 2) for Ga atoms in a trench: a) two Ga atoms splitting up two As dimers, b) forming a pair, thereby splitting only one As dimer, c) clustering of three Ga atoms.

Since already the clustering of two Ga atoms results in a large increase in the binding energy, the rate of formation of such pairs from a lattice gas of single diffusing Ga adatoms should exceed the rate of break-up of pairs even for a moderate supersaturation of Ga on the surface. Therefore, we conclude that the Ga adatom pair in the trench can be regarded as a stable nucleus in the sense of nucleation theory. Filling of the trenches will proceed by further attachment of Ga adatoms to these nuclei. In those regions of the surface where trench-filling has been completed, small Ga islands will also form in the next layer. Thus, the trench-filling triggers island growth on GaAs(001).

Upon further deposition of material, these islands start to grow. Quenched STM images have revealed small islands which do not yet show the (2×4) pattern [9]. After passing through this metastable intermediate state, eventually the islands restructure and display the trenches characteristic for the $\beta 2$ reconstruction. Larger islands have a very ragged shape, with longer protrusions in the $[\bar{1}10]$ direction. After growth interruption and annealing, they finally assume the shape of a rectangle elongated in the $[\bar{1}10]$ direction [29]. When thermo-

dynamic equilibrium is reached, the aspect ratio of these islands is equal to the ratio of the step energies per unit length along the [110] and [$\bar{1}$10] directions. Experimentally observed aspect ratios of islands grown on the GaAs(001) surface range from 2.4:1 [30] to 10:1 [31].

TABLE 2. Binding energy of Ga adatom clusters (in eV, relative to single adatoms in the reference site specified for each column, i.e., the lowest entry in Table 1). The star marks an empty site in the cluster.

		trench		top-layer	
		GGA	LDA	GGA	LDA
reference site		E^{II}_{trench}	E^{III}_{trench}	E^{II}_{top}	E^{II}_{top}
Ga * Ga *	a)	0.0	0.3	0.2	0.2
Ga Ga * *	b)	0.6	1.0	0.2	0.1
Ga Ga Ga *	c)	0.9	1.8	0.5	0.6

6. Growth in Step-Flow Mode

During the growth on a nominally flat GaAs(001) surface, the surface morphology will change continuously. The amplitude of diffraction peaks observed in RHEED, which can be used to monitor the morphology, shows damped oscillations. STM investigations of the surface at various stages of growth have suggested that oscillations of the step density are responsible for this behavior [32]. More recently, the RHEED oscillations were attributed to interference effects in elastic multiple scattering of electrons from the incomplete adlayer [33]. The completion of each new layer increases the surface order and, thus, results in a temporary recovery of the RHEED signal. When vicinal surfaces are used, the morphology of the surface as a whole may not change during growth, provided that the diffusion length of an adatom is larger than the average terrace width. In this case, growth proceeds predominantly through the attachment of material to the steps, which advance across the surface. Neave and co-workers [34] used the RHEED technique to study the transition to this so-called step-flow mode of growth, which occurs at sufficiently high temperatures and low Ga fluxes. Subsequently, the transition has been studied extensively by phenomenological Monte-Carlo simulations of growth [5,35]. A theoretical investigation of the conditions for step-flow growth has to take into account several microscopic processes [36].

Since at the transition point between the two regimes, attachment of mobile adatoms to the step edges competes with nucleation of islands on the terraces, the rates for these two processes must be known. We also need to know the diffusion tensor and its anisotropy.

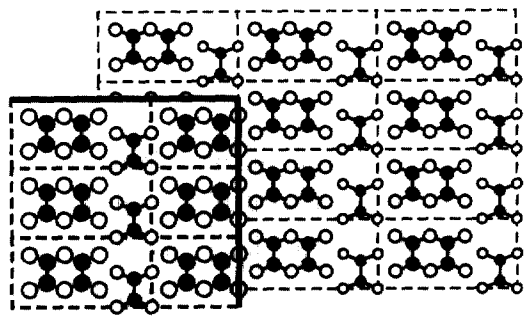

Fig. 4. Schematic illustration of two types of steps on GaAs(001). The lower left corner shows a terrace at a higher level bounded by an A step (thick vertical line) and a B step (thick horizontal line).

While *ab initio* information on the diffusivity of Ga adatoms is available (see sec. 4), knowledge of the geometrical and electronic structure of steps is a prerequisite for a microscopic understanding of the attachment process. There are two principal types of steps on a GaAs(001) surface (see Fig. 4 for illustration): A steps, which are found on surfaces slightly inclined towards the [110] direction, run parallel to the bond axis of the As dimers. B steps run perpendicular to the As dimers, and are found on surfaces miscut towards the [$\bar{1}$10] direction. STM images show that the (2×4) periodicity is maintained at the steps, i.e., kinks in the A steps have a minimum length of four lattice constants, while kinks in the B steps have a minimum length of two lattice constants. Generally, the surface height changes by a bi-layer at the step. Only at B steps, a region with a residual Ga layer on the lower terrace is observed in some cases [37].

We have investigated a large variety of possible microscopic structures for both the A and B steps by means of DFT calculations [38]. From the total energies we can calculate the energy of formation of a particular step at $T = 0\,\mathrm{K}$. Close to thermodynamic equilibrium, i.e., for annealed samples, the steps with the lowest formation energy occur most frequently. From our calculations, we find the general trend that A steps are less costly than B steps. The most favorable A steps are embedded between parallel As dimers both on the lower and the upper terrace. This atomic

structure avoids trenches, thus leading to a lower number of dangling bonds per unit area on vicinal surfaces inclined towards [110] than on the ideal GaAs(001) surface. For the B steps, we find it unavoidable to have extra dangling bonds due to the step. As a consequence, B steps are generally higher in energy than A steps. By analyzing the roughness of steps in STM images of vicinal surfaces, Heller, Zhang and Lagally [39] arrived at similar conclusions. They determined the ratio of step energies per unit length, β_B/β_A, to be 6:1. In our calculations, this ratio is of a similar order, but it also depends on the chemical potential of arsenic, i.e., on the annealing conditions.

Preliminary results show that the binding energy of Ga adatoms at certain step sites can be considerably higher than the binding energy in the trenches of the terraces. This finding gives microscopic support to the idea that steps can act as sinks for diffusing Ga adatoms. For sufficiently high adatom mobilities and low adatom concentrations, most adatoms will reach a step before they are captured by an island nucleating on the terrace. This will trigger the transition to the step-flow mode of growth.

References

1. E. Kapon, D.H. Hwang and R. Bhat, Phys. Rev. Lett. **63**, 430 (1989); F.S. Turco, S. Simhony, K. Kash, D.M. Hwang, T.S. Ravi, E. Kapon and M.C. Tamargo, J. Cryst. Growth **104**, 766 (1990).
2. H.T. Dobbs, D.D. Vvedensky, A. Zangwill, J. Johansson, N. Carlsson and W. Seifert, Phys. Rev. Lett. **79**, 897 (1997).
3. N. Moll, E. Pehlke and M. Scheffler, Phys. Rev. B **58**, 4566 (1998).
4. S.V. Ghaisas and A. Madhukar, SPIE Proceedings **944**, 16 (1988).
5. T. Shitara, D.D. Vvedensky, M.R. Wilby, J. Zhang, J.H. Neave and B.A. Joyce, Phys. Rev. B **46**, 6815 (1992); Phys. Rev. B **46**, 6825 (1992).
6. F. Große, R. Zimmermann, A. Kley and M. Scheffler, to appear in *Proceedings of the 24th International Conference on the Physics of Semiconductors*, World Scientific, Singapure (1998).
7. C. Heyn and M. Harsdorff, Phys. Rev. B **55**, 7034 (1997).
8. P. Smilauer, M.R. Wilby and D.D. Vvedensky, Phys. Rev. B **47**, 4119 (1993).
9. M. Itoh, G.R. Bell, A.R. Avery, T.S. Jones, B.A. Joyce and D.D. Vvendensky, Phys. Rev. Lett. **81**, 633 (1998).
10. D.M. Ceperley and B.J. Alder, Phys. Rev. Lett. **45**, 566 (1980); J.P. Perdew and A. Zunger, Phys. Rev. B **23**, 5048 (1981).
11. J.P. Perdew, K. Burke and M. Ernzerhof, Phys. Rev. Lett. **77**, 3865 (1996).
12. M.C. Payne, M.P. Teter, D.C. Allan, T.A. Arias and J.D. Joannopoulos, Rev. Mod. Phys. **64**, 1045 (1992).
13. M. Bockstedte, A. Kley, J. Neugebauer and M. Scheffler, Comput. Phys. Commun. **107**, 187 (1997); see also http://www.fhi-berlin.mpg.de/th/fhimd/code.html.
14. C.T. Foxon and B.A. Joyce, Surf. Sci. **64**, 293 (1977).

15. S.Y. Karpov and M.A. Maiorov, Surf. Sci. **344**, 11 (1995).
16. L. Däweritz and R. Hey, Surf. Sci. **236**, 15 (1990).
17. Q.-K. Xue, T. Hashizume and T. Sakurai, Prog. Surf. Sci. **56**, 1 (1997).
18. J.E. Northrup and S. Froyen, Phys. Rev. Lett. **71**, 227 (1993); Phys. Rev. B **50**, 2015 (1994).
19. N. Moll, A. Kley, E. Pehlke and M. Scheffler, Phys. Rev. B **54**, 8844 (1996).
20. A. Kley, P. Ruggerone and M. Scheffler, Phys. Rev. Lett. **79**, 5278 (1997).
21. K. Shiraishi, Thin Solids Films **272**, 345 (1996).
22. C.T. Foxon and B.A. Joyce, Surf. Sci. **50**, 434 (1975).
23. C.G. Morgan, P. Kratzer and M. Scheffler, Phys. Rev. Lett., submitted.
24. K. Shiraishi and T. Ito, Surf. Sci. **357–358**, 451 (1996); Phys. Rev. B **57**, 6301 (1998).
25. A.R. Avery, C.M. Goringe, D.M. Holmes, J.L. Sudijono and T.S. Jones, Phys. Rev. Lett. **76**, 3344 (1996).
26. H. Farrel, J.P. Harbison and L.D. Peterson, J. Vac. Sci. Technol. B **5**, 1482 (1987).
27. A.R. Avery, H.T. Dobbs, D.M. Holmes, B.A. Joyce and D.D. Vvedensky, Phys. Rev. Lett. **79**, 3938 (1997).
28. P. Kratzer, C.G. Morgan and M. Scheffler, to be published.
29. T. Ide, A. Yamashita and T. Mizutani, Phys. Rev. B **46**, 1905 (1992).
30. V. Bressler-Hill, R. Maboudian, M. Wassermeier, X.-S. Wang, K. Pond, P.M. Petroff and W.H. Weinberg, Surf. Sci. **287–288**, 514 (1993).
31. E.J. Heller and M.G. Lagally, Appl. Phys. Lett. **60**, 2675 (1992).
32. J. Sudijono, M.D. Johnson, C.W. Snyder, M.B. Elowitz and B.G. Orr, Phys. Rev. Lett. **69**, 2811 (1992); J. Sudijono, M.D. Johnson, M.B. Elowitz, C.W. Snyder and B.G. Orr, Surf. Sci. **280**, 247 (1993).
33. W. Braun, L. Däweritz and K.H. Ploog, Phys. Rev. Lett. **80**, 4935 (1998).
34. J.H. Neave, P.J. Dobson, B.A. Joyce and J. Zhang, Appl. Phys. Lett. **47**, 100 (1985).
35. D.D. Vvedensky and S. Clarke, Surf. Sci. **225**, 373 (1990).
36. Y. Kajikawa, M. Hata, T. Isu and Y. Katayama, Surf. Sci. **265**, 241 (1992).
37. A.R. Avery, D.M. Holmes, T.S. Jones, B.A. Joyce and G.A.D. Briggs, Phys. Rev. B **50**, 8098 (1994).
38. P. Kratzer and M. Scheffler, unpublished.
39. E.J. Heller, Z.Y. Zhang and M.G. Lagally, Phys. Rev. Lett. **71**, 743 (1993).